Pergamon

LINEPAK: ALGORITHMS FOR MODELING SPECTRAL TRANSMITTANCE AND RADIANCE

Larry L. Gordley, Benjamin T. Marshall, and D. Allen Chu

G&A Technical Software Inc., 28 Research Drive, Hampton, VA 23666, U.S.A.

Abstract—A set of subroutines has been written for use in developing spectral models, with emphasis on the Earth's atmosphere. Features include rapid calculation of absorption cross section, radiance and transmission spectra for multiple gases and multiple paths. The routines are designed to allow user control of model geometry, line shape functions, band models, atmospheric layering, and spectral resolution. Numerical techniques and applications are described with examples that include a simulated limb scan retrieval and comparison to other codes.

1. INTRODUCTION

As research in atmospheric science accelerates, both observation and model complexity increases. Measurements are being taken in the lab and from ground, balloon, aircraft, and spacecraft. Researchers are developing a variety of observing systems and are being supported by investigations into the fine details of energy state transitions. Concurrently, advances in computer technology are improving the ability to support these activities with rigorous calculations.

Our objective in developing the LINEPAK subroutine library was to create a set of tools for quickly producing detailed models of spectroscopic measurements of the atmosphere. The routines were designed to accommodate changes in spectroscopic data, viewing geometry and model resolution without code alteration or substantial loss of efficiency. We simplified both use and understanding while providing speed and utility. Cross section, optical path, and integration routines can be used separately or in concert to allow custom modeling of complicated multiple angle observations.

The LINEPAK library is being used in the operational data processing of HALOE (Halogen Occultation Experiment) data, and for the development of transmission tables for CLAES (Cryogenic Limb Array Etalon Spectrometer) and ISAMS (Improved Stratospheric and Mesospheric Sounder). All three instruments are on the UARS (Upper Atmosphere Research Satellite). The library has also been used to simulate rigorous high resolution retrievals for two instruments proposed for EOS (the Earth Observation System), SAFIRE (Spectroscopy of the Atmosphere using Far Infrared Emission), and the MLS (Microwave Limb Sounder). In addition, the library is being used to simulate high resolution spectra observed from ground, aircraft, and satellite for a variety of other instruments making measurements throughout the near and far infrared.

Numerous advances have been made in computer algorithms which perform these calculations (Clough et al,[1] Edwards[2]), but many researchers have still resorted to developing their own. The available algorithms tend to be difficult to configure to specific applications, or reliable modifications to equations, constants, resolution, and other physical factors are difficult to perform. LINEPAK overcomes such problems, providing the researcher with tools that can be quickly configured for a variety of measurement scenarios and that can easily incorporate changes to the equations and physical factors used in the spectral modeling.

2. THE PROBLEM

Modern instruments require exact characterization of the sensed radiation field over a variety of viewing directions. The atmosphere is a heterogeneous medium that rapidly changes character as a function of space (view direction), time, and spectral band-region. Fast rigorous calculations, sufficient for modeling these conditions, require tedious but efficient numerical procedures for constructing raypaths and spectra. In describing numerical procedures in LINEPAK, we refer to segments, cells, and sections. Our definition of a "segment" is a finite piece of an optical path, typically a raypath through a user defined atmospheric layer. A "cell" is defined as a homogeneous column of gas at a constant temperature and pressure, analogous to a cell in a laboratory. When discussing "sections" we are referring to finite pieces of the spectral band-region being modeled.

Radiance and transmission spectra originating from some path through a heterogeneous medium can be accurately modeled with a sequence of homogeneous cells. Finite spatial fields are estimated from multiple ray calculations at different viewing angles. If the model requires finite spectral width, each ray is calculated for multiple monochromatic values to allow spectral integration.

Calculating measured radiance at wavenumber v for a perfectly resolved line of sight, requires numerical evaluation of Eq. (1).

$$L(v) = F(v)\left\{ B_b(v)\tau(v, s_b) - \int_0^{s_b} B[v, T(s)]\frac{\partial \tau(v, s)}{\partial s}\, ds \right\} \qquad (1)$$

where $L(v)$ is response to monochromatic radiance, v is wavenumber, s is distance from the instrument along the line of sight, s_b is position of a background source, $F(v)$ is instrument band pass evaluated at wavenumber v, $T(s)$ is temperature along the line of sight, $B(v, T)$† is emission source function, $\tau(v, s)$ is the transmission at wavenumber v from the instrument to position s along the line of sight, $B_b(v)$ is background source function (e.g., sun, star, or laboratory source). The transmission τ is a function of many parameters (e.g., temperature, pressure, species concentration) with varying distribution along the path. (To simplify notation we do not include all dependent variables in this and other equations). The evaluation of τ along an optical path dominates the calculations required to solve Eq. (1).

Spectra for a single ray are modeled by partitioning the ray into segments. Each segment is approximated as a cell with constant temperature, pressure, and mixing ratios. The cross section spectra are calculated by proceeding with one spectral section for all cells before continuing to the next section. To perform fast multiple path calculations, the number of cell conditions necessary to model all segments for all rays must be minimized. The cross sections must be efficiently calculated, for all absorbers and cells, with a gridding scheme that allows straightforward and fast integration along a raypath.

The four primary functions of the LINEPAK library used to accomplish these tasks are: (1) sorting and storing line transition parameters; (2) atmospheric path modeling; (3) calculation of absorption cross section spectra; (4) calculation of transmission and radiance fields, both monochromatic and spectrally integrated. These tasks are performed by separate subroutines called by the user's program. They can be used independently or together. The following describes the techniques used in the LINEPAK routines.

2.1. Monochromatic transmission

The fundamental building block of a spectral model is the monochromatic ray transmission value τ for a single gas over a homogeneous cell. From Beer's law

$$\tau_g(v) = \exp[-u_g \sigma_g(v)]$$

---

†B, commonly used to indicate the Planck function, is used to symbolize the source function throughout this paper. Since our discussions are of LTE (Local Thermodynamic Equilibrium) calculations, the association of this term to the Planck function is intentional. LINEPAK has recently been extended to allow non-LTE calculations, but these extensions are not discussed.

where v is wavenumber (cm^{-1}), u_g is optical mass (molecules/cm^2) for gas g, $\sigma_g(v)$ is cross section at wavenumber v for gas g (cm^2/molecule). For multiple gases the equation is

$$\tau(v) = \prod_{g=1}^{m} \tau_g(v) = \exp\left[-\sum_{g=1}^{m} u_g \sigma_g(v) \right] \tag{2}$$

where m is number of gases. For multiple cells and multiple gases, the equation is

$$\tau(v) = \prod_{j=1}^{n} \prod_{g=1}^{m} \tau_{jg}(v) = \exp\left[-\sum_{j=1}^{n} \sum_{g=1}^{m} u_{jg} \sigma_{jg}(v) \right] \tag{3}$$

where n is the number of cells and j is the individual cell.

Rapid evaluation of $\tau(v)$ becomes the most important numerical task. This requires efficient procedures for calculating u and σ for multiple segments in ways that simplify integration over wavenumber. The LINEPAK code calculates cross section functions $\sigma_{jg}(v)$ for a set of cell conditions. The conditions can be generated by either LINEPAK or user routines. The cross sections are stored in a form that allows efficient spectral and spatial integration using LINEPAK or user routines (as described in Sec. 3) for modeling optical paths.

2.2. Raypath modeling

LINEPAK tools were designed for Earth remote sensing applications, but can be used for other planetary atmospheres. The use of LINEPAK allows specification of the atmospheric layering with an array of altitude values, which defines the boundaries of ray segments.

Figure 1 illustrates how ray models are constructed. Inputs are platform altitude, zenith angles of observation and layer boundary altitudes. For limb views, observation angles must (or are forced to) have apparent tangent heights coinciding with layer boundaries. Each raypath is represented by a complete limb path or a section of a limb path, including refraction effects. Note that for nadir or vertical views, the tangent location is earth center. (See Sec. 6 for a more detailed explanation.)

3. CROSS SECTION CALCULATIONS

Cross section calculations in a line-by-line code can dominate the time and complexity. From Eqs. (2) and (3), we see that each gas can be treated independently, then multiplied with the
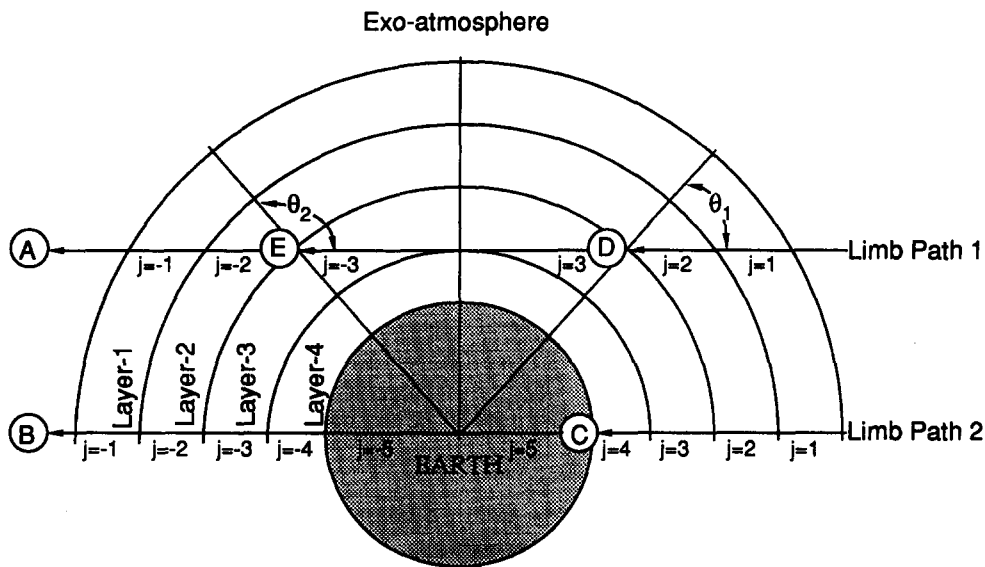

Fig. 1. General ray geometry. (A) Represents space based observation along a limb path tangent to the bottom edge of layer 3. (B) Represents observation from space of the Earth's surface along a path normal to the Earth's surface. (C) Represents ground based observation along a path normal to the Earth's surface. (D) Represents an observation from within the atmosphere at a zenith angle θ_1. (E) Represents an observation from within the atmosphere at a zenith angle θ_2.

appropriate optical mass, and summed with other gas contributions and other cells. Therefore, it is necessary to understand details of only the single gas model.

3.1. Single gas single cell cross sections

The single gas molecular absorption cross section is a function of temperature, wavenumber, pressure, gas volume mixing ratio and constants associated with all contributing line transitions. Cross section contributions at temperature T, due to a single transition i centered at v_i, can be written as the product of a transition line strength $S_i(T)$ and a line shape profile $g(v, v_i)$. The monochromatic cross section at temperature T and wavenumber v is written as

$$\sigma(v, T) = \sum_i S_i(T) g(v, v_i).$$

We define

$$g(v, v_i) = \frac{v}{v_i} \frac{\tanh(hcv/2kT)}{\tanh(hcv_i/2kT)} f(v, v_i)$$

where f is the broadening function and is a function of pressure, temperature, gas volume mixing ratios, transition and often other factors.

We note that in regions of dense spectra (e.g., the CO_2 Q branch), using simple transition summation to determine τ may not be valid due to quantum state mixing (line mixing). However, an accurate approximation of this effect has been achieved using the standard summation model by incorporating non-physical line broadening functions (Rinsland and Strow[3]). Accurate use of the LINEPAK code requires that transition summation be adequate for the default line broadening functions or that the user supply broadening functions that adequately model mixing effects under the summation assumption. (See Sec. 7.2)

For the HITRAN (Rothman et al[4]) data set, the line strength at a reference temperature T_0 for a transition centered at v_i is defined by

$$S_i(T_0) = d_i I_a \frac{8\pi^3}{3hc} v_i \frac{\exp(-hcE_L/kT_0) - \exp(hcE_u/kT_0)}{Q_v(T_0)Q_R(T_0)} R_i 10^{-36}$$

where d_i is nuclear spin degeneracy of the lower state, I_a is isotopic abundance, E_L is lower state energy (cm^{-1}), E_u is upper state energy (cm^{-1}), h is the Planck constant, k is the Boltzmann constant, Q_v is the vibrational partition function, Q_R is the rotational partition function, c is the speed of light, T_0 is reference temperature in Kelvin, R_i is transition intensity (Debye^2), and 10^{-36} is a conversion factor from Debye^2 to cgs units. The upper state energy is the sum of lower state energy and the transition energy hcv_i. For an arbitrary temperature T, the cross section is rewritten as:

$$\sigma(v, T) = \sum_i \frac{\exp(-hcE_L/kT)}{\exp(-hcE_L/kT_0)} \frac{[1 - \exp(-hcv_i/kT)]}{[1 - \exp(-hcv_i/kT_0)]} \frac{Q_v(T_0)Q_R(T_0)}{Q_v(T)Q_R(T)} S_i(T_0) g(v, v_i).$$

The first term inside the summation is the ratio of the Boltzman factor at ambient temperature to reference temperature. The second term is the ratio of the stimulated emission at ambient temperature to reference temperature. The rotational and vibrational partition functions are calculated as a total partition (Gamache et al[5]). Along with coefficients for calculating total partition, gas constants such as molecular weight and isotopic abundance are tabulated in a data file read by the routines, allowing these constants to be altered.

3.2. The broadening function $f(v, v_i)$

Different broadening functions may be required for different transitions. For example, the Voigt function in the i.r. region and the van Vleck–Weisskopf (van Vleck and Weisskopf[6]) function in the microwave region. For line mixing calculations, the imaginary part of the complex probability function must be included (Rosenkranz[7]).

LINEPAK is designed to accommodate a variety of broadening functions. By modifying the line transition file, lines can be assigned specific broadening functions (see Sec. 3.2.2.). The code includes three broadening functions: (1) a table look-up Voigt, (2) the Drayson[8] Voigt algorithm (the default

broadening function), and (3) a line mixing approximation (the line mixing calculation uses a complex Voigt routine based on Humlicek[9]). The Voigt function is sufficient for most atmospheric applications. The Voigt broadening function, a convolution of Doppler and Lorentz broadening is defined by

$$f(v, v_i) = \frac{1}{\alpha_{Di}\sqrt{\pi}} K(x_i, y_i) \tag{4}$$

where

$$K(x_i, y_i) = \frac{y_i}{\pi} \int_{-\infty}^{+\infty} \frac{\exp(-t^2)}{(x_i - t)^2 + y_i^2} \, dt;$$

$$y_i = \frac{\alpha_{Li}}{\alpha_{Di}}; \quad x_i = \frac{v - v_i}{\alpha_{Di}}.$$

α_{Li} is Lorentz halfwidth (cm^{-1}) at half maximum for transition i, α_{Di} is Doppler halfwidth (cm^{-1}) at $1/e$ of maximum. The Lorentz halfwidth at pressure P and temperature T is given by the relation (dropping the i subscript for now)

$$\alpha_L = \alpha_L^0 \left(\frac{P}{P_0} \right) \left(\frac{T_0}{T} \right)^\gamma$$

where P_0 and T_0 are the pressure and temperature at the reference state (1 atm and 296 K for HITRAN lines), α_L^0 is the Lorentz halfwidth at P_0 and T_0, and γ is an exponent used to model temperature dependence. The Lorentz halfwidth includes both foreign and self broadened components so that

$$\alpha_L^0 = (1 - q)\alpha_{Lf}^0 + q\alpha_{Ls}^0$$

where α_{Lf}^0 and α_{Ls}^0 represent foreign broadening and self-broadening and q is the volume mixing ratio of the absorber. The Doppler width factor for transition i is

$$\alpha_{Di} = \frac{v_i}{c} \sqrt{\frac{2kT}{m}}$$

where m is the mass of the molecule. (Note that $\sqrt{\ln 2}$ is not included in this equation since we are using halfwidth at $1/e$ maximum.)

3.2.1. Broadening function construction. Fast line by line calculations demand rapid evaluation of broadening effects. There are several algorithms (with varying accuracy and speed) for calculating the Voigt and related functions (Schreier[10]). For optimum speed, these functions must be augmented with a scheme that minimizes their use. Most schemes not only simplify the wing calculations, but reduce the resolution and therefore the number of function evaluations in the wings. However, reduced resolution complicates the integration and/or requires interpolation to a higher resolution grid. Since the wing distances that must be included are typically much greater than the width of regions near line center which require Voigt-like calculations, the interpolation to a finer grid can dominate the computational time.

To overcome the interpolation barrier, Clough[1] models the cross section spectra using up to five additive functions at successively lower resolution. This allows the contribution of line wings from all lines to be distributed among five different spectra, each spectrum interpolated only once to a finer grid, then added together to create the total spectra. In effect, this gives nearly the equivalent of one coarse-to-high density interpolation across the entire bandpass instead of one for each line transition. Although the technique makes a dramatic improvement in spectral modeling speed, the use of functions tailored to modeling a specific broadening function limits the ability to alter either resolution or broadening physics. A conceptually similar scheme is used in LINEPAK, but only two functions are employed. The method allows easy change of resolution and broadening functions (including asymmetric functions), and induces virtually no loss of accuracy while avoiding the interpolation barrier described above.

Figure 2 illustrates the LINEPAK broadening function scheme (shape is not to scale). The function is divided into three regions labeled I, II, and III. For the default line shape, a Voigt calculation is performed in region I and a Lorentz function is used for regions II and III. For user
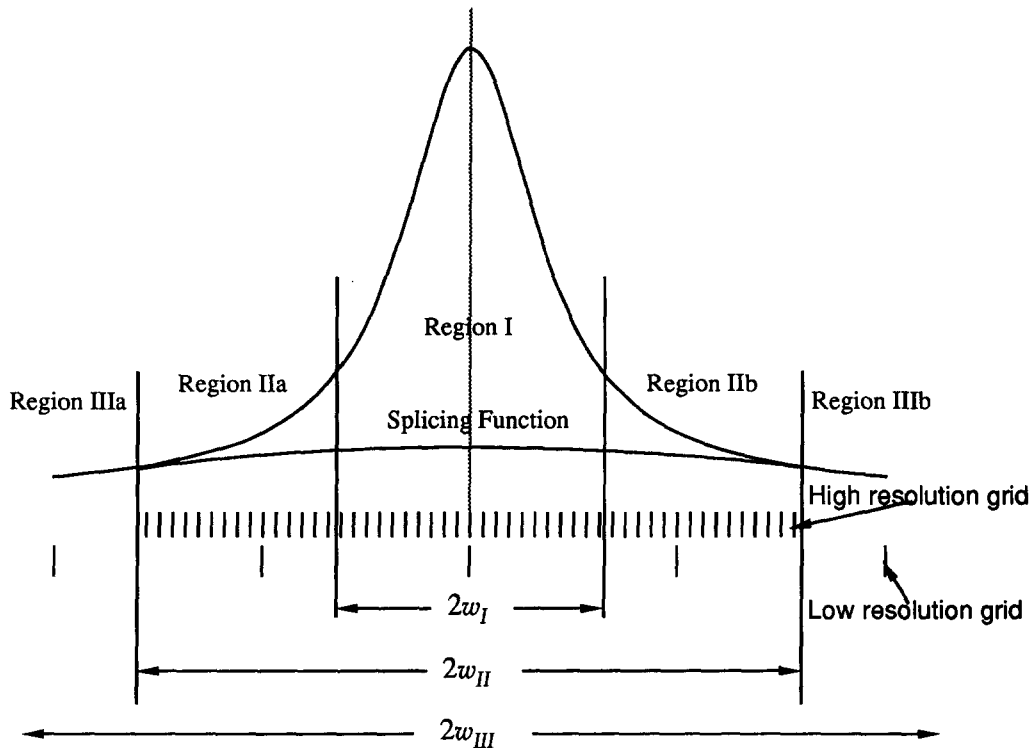
Fig. 2. Broadening function construction. Region III extends into the far wings of the line but is constrained to be less than a user defined width. Also, if $w_{III} \leqslant w_{II}$ then low resolution is not calculated. $w_I = a\alpha_D$, $w_{II} = b\alpha_V$, and $w_{III} = c\alpha_L$. w_I, w_{II} and w_{III} are distances from line center. Default values for a, b, and c are 20, 30, and 5000. Note: the grid points need not coincide with region boundaries.

supplied functions, the region is identified in the function call, allowing efficiency considerations to be built into the user code. High resolution spectra are calculated only over regions I and II at a point spacing of $\delta\alpha_V$, where $\alpha_V = (\alpha_{Lm} + \alpha_D)$. α_{Lm} is the smallest pressure broadening halfwidth, for the relevant gas, of all lines considered. The value of δ can be specified (default is $\delta = 0.2$ which limits integration error to less than 0.3%). The point spacing for the low resolution spectra calculated over the entire line shape function is $\epsilon\delta\alpha_V$, where ϵ can be set by the user (default, $\epsilon = 10.0$). The Lorentz function is the default used in region III. A third order polynomial is used to splice region IIIa with IIIb, insuring continuous low resolution spectra. This splicing function is subtracted from the high resolution values to accommodate later interpolation and summation of the high and low resolution spectra.

Figure 3 shows the result of the third order splicing fit on a line shape used to approximate line mixing. The ordinate is relative to a line center value of 0.0045. For most cases the splicing function is very small. It induces error less than that caused by finite resolution. The third order polynomial allows simple installation of asymmetric broadening funtions. The fit is achieved by using the $\pm w_{II}$ position values and first derivatives as boundary conditions.

This method of construction allows easy control of resolution and simplified installation of different functions (Sec. 3.2.2). Figure 4 shows the maximum error in the Voigt function evaluation due to various values of a and y (a determines where the transition from Voigt to Lorentz occurs and y is the ratio of Lorentz to Doppler halfwidth). Figure 5 shows the maximum error due to linear interpolation in region III for various ϵ and b values (ϵ determines the ratio of coarse to fine point spacing and b determines the distance from line center where the resolution switches). The default values are shown to cause less than 0.4% error at the maximum error locations (between points). Considering how far down on the wings these errors occur, error in integrated emission or line width due to these approximations is under 0.1%. The user can reduce these errors further by increasing a and/or b.
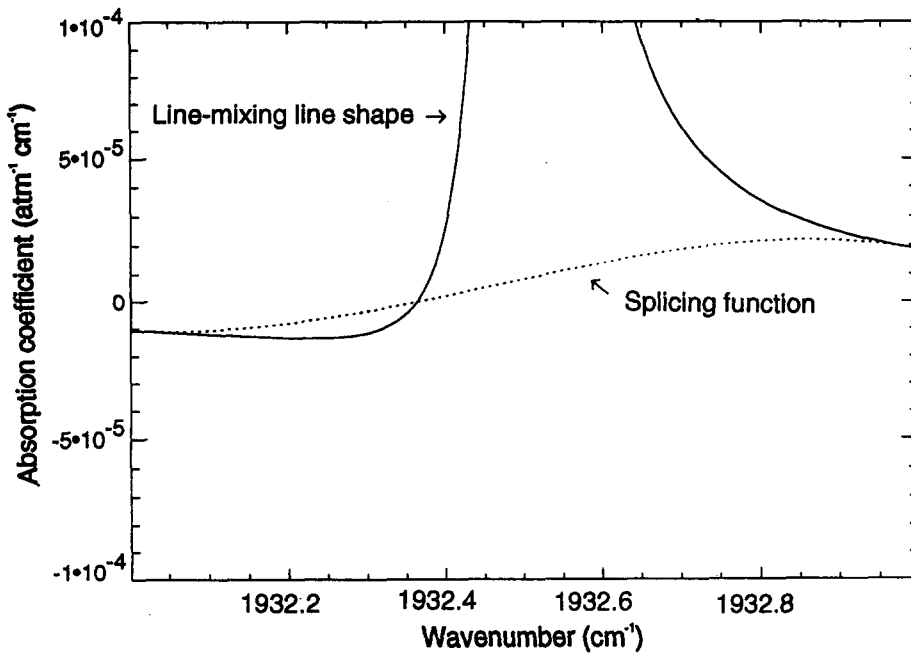
Fig. 3. Asymmetric broadening function construction—line mixing example.

3.2.2. Adding broadening functions.

In addition to the broadening functions included with LINEPAK, the code allows the option of supplying broadening routines to be used on selected line transitions. This is accomplished by linking routines that follow a prescribed interface and define the K function (see Sec. 3.2), and by adding information to the transition line file. Each transition line chosen for a different line shape must have an additional record inserted that contains broadening function identification information and additional constants (if necessary) to be passed to the selected broadening routine. In effect it would be possible to assign a custom line shape to each transition.

3.3. Transition line data

The line transition data must be supplied on a file in a HITRAN[4] format, with previously described extensions (see Sec. 3.2) when additional broadening functions are used. The LINEPAK
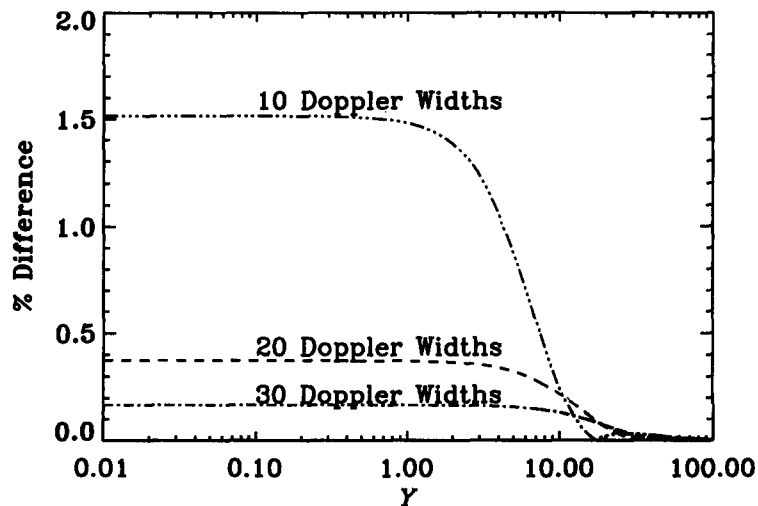

Fig. 4. Voigt vs Lorentz differences. The difference between Voigt and Lorentz functions at 10, 20, and 30 Doppler widths from line center as a function of y.
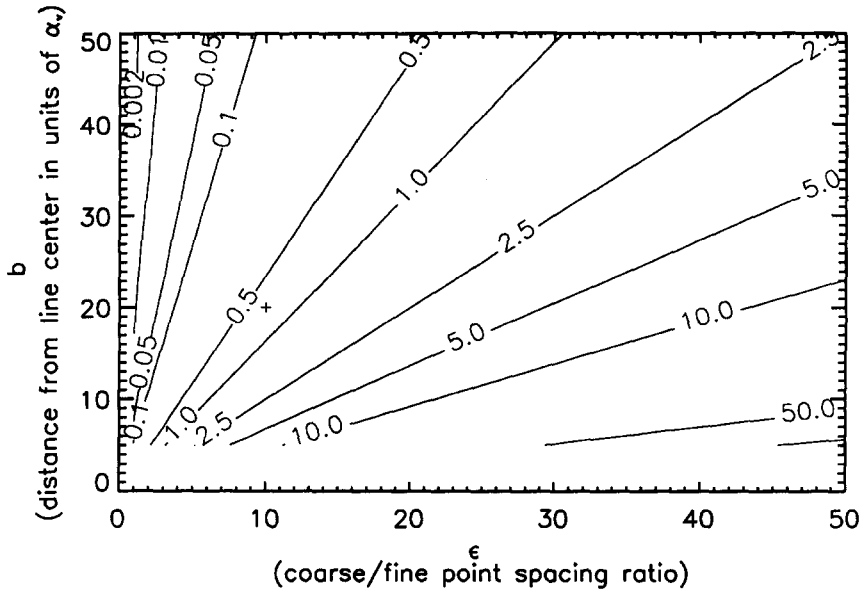
Fig. 5. Maximum single point interpolation error (percent) in region III. LINEPAK defaults of $\delta = 0.2$ and $\epsilon = 10.0$ are used (error at default beginning of region III is given by $+$).

code reads the data for the requested gases and spectral interval and sorts the data by gas. This sorted line data is placed in arrays, allowing easy manipulation for spectral analysis, such as the inference of line constants from lab spectra. The code also provides the option of having the data written to direct access files, allowing use of large line sets on machines with limited memory.

3.4. Weak line and distant line cut-offs

The computational speed of cross section calculations can vary by orders of magnitude, depending on the degree to which weak lines and line wings are included. This can be adjusted to optimize the balance between speed and accuracy. At any spectral position, the total cross section for a gas is the sum of the contribution from all transitions. Usually the contribution from distant lines approaches zero as the distance increases. The code has four simple adjustable criteria for determining the cutoff wavenumber distance.

(1) A maximum distance, *WNMAX*, in wavenumber. The contribution from lines more distant than *WNMAX* cm^{-1} are not included.

(2) Maximum number of Lorentz halfwidths N_L. The contribution from lines greater than $\alpha_L N_L$ from a spectral position are not considered. This criteria is not allowed to be less than $\alpha_D N_D$, to accommodate low pressures. N_D has a default value of 6, but can be assigned by the user.

(3) A minimum optical depth, *TDLMT*, for the center of a Doppler broadened line. Lines that would contribute less than *TDLMT* in optical depth at line center, if they were only Doppler broadened, are not included.

(4) A minimum optical depth, *ODMIN*, for line wing contribution. Line wings are cut off where optical depth is less than *ODMIN*.

The optical depth calculations require that an optical mass value be specified for each cell condition. If not supplied, the optical depth criteria are not considered.

Although signficant additional speed can be gained by combining weak lines under optically thin conditions, we do not incorporate such procedures. High resolution and low noise measurements are limiting the appeal and utility of these methods. If such methods are desired, the line data must be condensed by the user.

3.5. Band models

LINEPAK can be used to calculate cross sections from band model data, for any or all gases, using band model functions supplied by the user, or using one of the three models included. All band model coefficient data required for a single use of LINEPAK are contained in one file, and include an identifier to allow assignment of the proper function. An interface convention specifies parameters that are passed to the functions. These include wavenumber, cell temperature, cell pressure, gas volume mixing ratio, and all band model data including spectral grid information.

Any number of spectral bands can be defined. Each is included as a separate block of data on an evenly spaced spectral grid. Cross sections are calculated at the required resolution by interpolation between the grid points defined in the data file. Band model cross sections can be calculated separately or in addition to line transition cross sections. The three models supplied with the LINEPAK library are: (1) a simple exponential band model that does not allow pressure dependence, (2) a band model used to calculate the H_2O continuum using band model data derived from Clough et al,[11] and (3) a band model to calculate O_2 pressure induced continuum using data derived from Orlando et al.[12]

4. SPECTRAL RESOLUTION, SECTIONING, AND OTHER NUMERICAL CONSIDERATIONS

The efficient modeling of multiple raypaths for broadbands and multiple gases in one execution demands simple calculations when possible and a minimum number of cross section calculations. Integration over wavenumber is expedited by using equally spaced data on a common grid, which allows integration without interpolation using vector addition.

Cross section calculations for each cell condition (i.e., pressure, temperature, gas volume mixing ratio) are performed on a maximally and equally spaced grid. Line broadening functions are evaluated at the exact grid point positions consistent with each line transition. Point spacing Δv_j for cell j is determined by $\Delta v_j < \delta (\alpha_{Lmj} + \alpha_{Dj})$ and $n\Delta v_j = \Delta w$, where δ is a specified input factor (default = 0.2), α_{Lmj} is the minimum Lorentz halfwidth of all lines considered for the gas and cell condition j, α_{Dj} is the Doppler halfwidth for cell condition j, n is a whole integer number, and Δw is the width of a spectral section, Δs, less one high resolution element width (see Fig. 6).
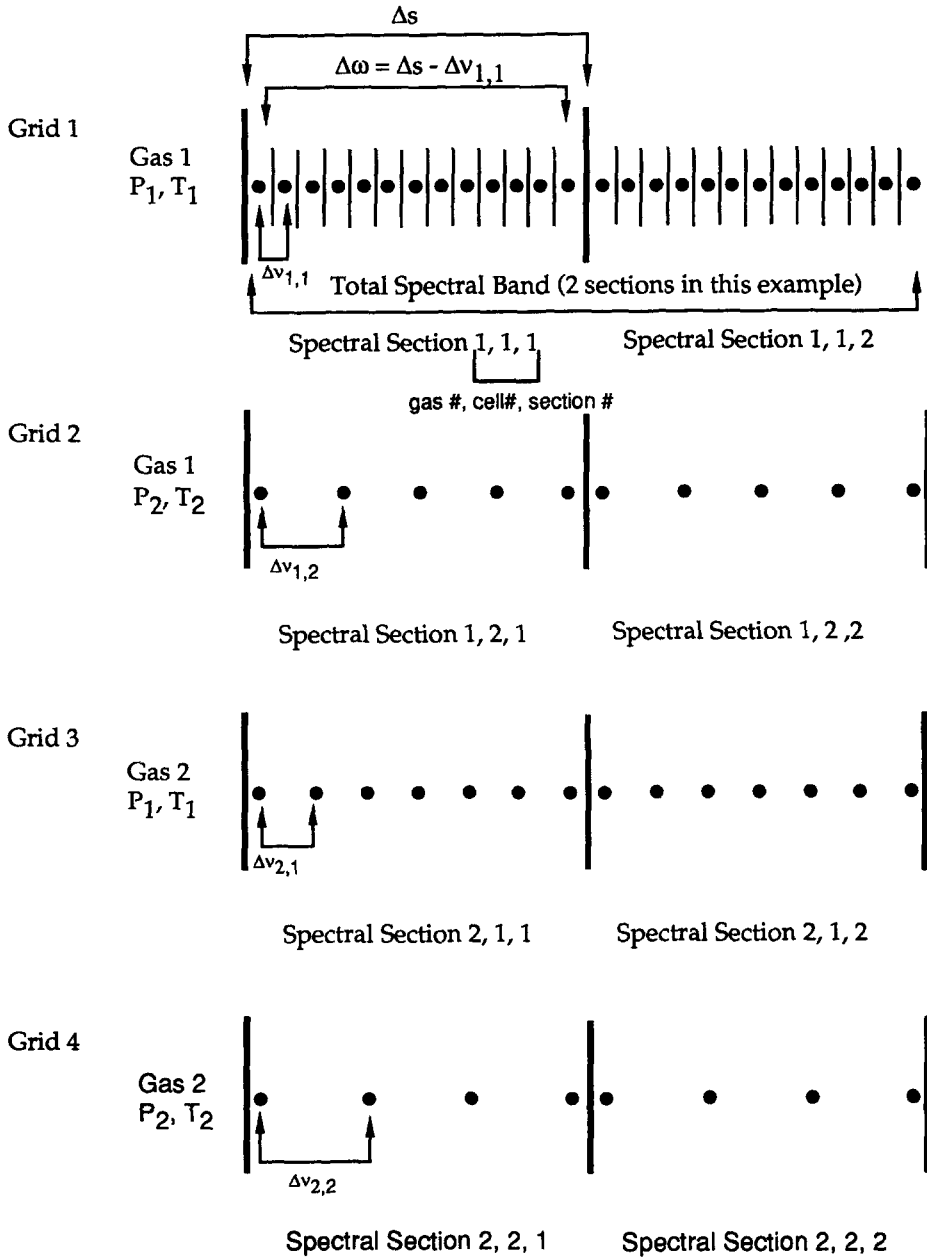
Figure 6 is a conceptual depiction of the numerical strategy used in creating and integrating spectral grids. The figure is for an example case of 2 gases and 2 pressure-temperature combinations (cells). This requires 4 grids, each optimized to require a minimum of points. If the array size supplied by the user is insufficient to hold all the grids (in this case 4) at the highest resolution (in this case the spacing of grid 1), the code subdivides the spectral interval into enough equal length sections to allow one section for each grid to reside in memory simultaneously. The initial call to the cross section routine calculates the first section for each grid, with subsequent calls calculating successive sections. This allows multiple paths that require many spectral grids to be calculated and integrated with small memory machines.

The point spacing for the finest grid in the example is used as the base grid. For the base grid, points are calculated at the center of each Δv wide element. For all other grids, points are equally spaced, with the first and last point of each subsection coinciding with the first and last points of the base grid subsection. This allows interpolation of all spectra to the base spacing without extrapolation or special end point considerations. Once all spectra are at the base point spacing, integration and section summation become seamless and trivial. With points evenly spaced, interpolation is very efficient, requiring about one floating point operation (1 multiply plus 1 add) per point, and easily vectorized.

Using cross sections for all cells and all gases on the same minimum point spacing may not allow the fastest possible integration along a ray. Schemes summing the lowest resolution cells first, working out to the higher resolution, are faster. However such schemes limit flexibility in retrieval iteration, often induce interpolation and endpoint bugs and are only marginally faster for most uses. With advances in hardware capabilities we have opted for more conceptually clean and flexible numerical procedures when possible. We avoid higher order fits for similar reasons.

If more detail and accuracy are needed, LINEPAK can be run on a finer grid, since the user has complete control of both spatial and spectral resolution. Using linear interpolation also removes the liablity of poor fits.

A final point involves utility. To achieve the goal of modularity, modules must be cleanly de-coupled to allow independent use. The cross sections and path partitioning parameters can be easily understood and used independently by higher level code. This is best facilitated by conceptually simple schemes.

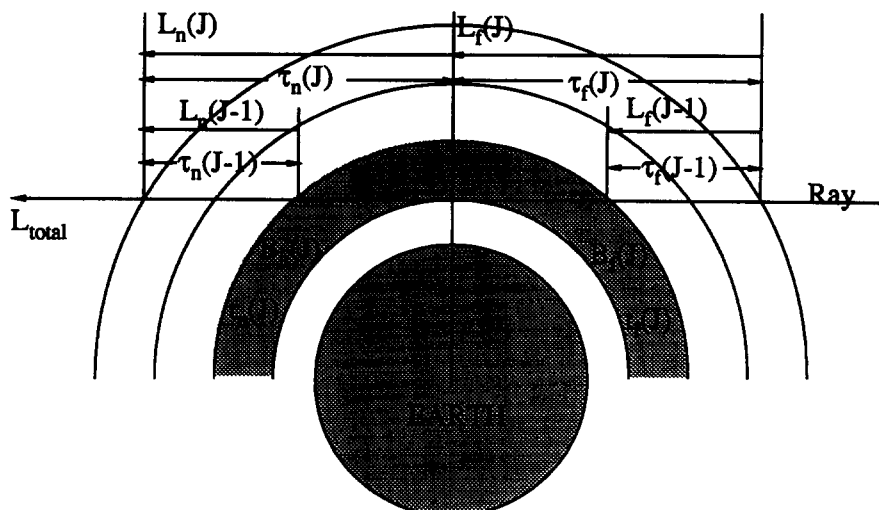Fig. 6. Spectral gridding methodology.

Fig. 7. Along-path integration procedure. Top of the atmosphere is modeled with one layer. Efficient limb path iteration requires integration from outside in.

5. ATMOSPHERIC PATH MODELING

For atmospheric applications, continuously varying parameters are accurately represented along a refracted path using a set of homogeneous cells. To model the effective characteristics of each segment with a homogeneous cell, mass-weighted quantities are used to define the basic parameters. Optical mass and mass weighting of all quantities are accurately calculated along the simulated refracted path. All segment associated values are available in arrays for use in higher level modules. For more details, see Marshall et al[13] Section 3, this issue.

5.1. General mass model

The mass model used by LINEPAK calculates integrated segment parameters with linear equations which use pre-calculated moments of column air mass. Integrated parameters for segment Δs are assumed to take the general form

$$A = \int_{\Delta s} \rho(s)[a + bz(s) + cz(s)^2]ds \qquad (5)$$

where: $\rho(s)$ is atmospheric density at s, $z(s)$ is altitude at s as referenced to the segment medium altitude, and a, b and c are simple polynomial coefficients calculated directly from the state vectors. Column air mass moments are determined by separately integrating the terms $\rho(s)$, $\rho(s)z(s)$, and $\rho(s)z(s)^2$ in Eq. (5) for each segment. The values for A can be calculated by using these moments in simple linear equations. A change in volume mixing ratio will change only a, b, and c, which can be quickly re-evaluated and used with the pre-calculated moments for very accurate updates of integrated columns and mass-weighted parameters. This mass model is more completely discussed (including refraction effects) in Marshall et al[13] Section 5, this issue.

5.2. Alternative mass models

The most time consuming task in line by line spectral models is the calculation of cross sections for each cell for every ray modeled (required by the general mass model). For multiple limb path applications the computational requirements for this model can often overwhelm available computing resources. To reduce the calculations necessary for such applications, one of two optional models may be selected.

The first optional model represents each raypath with a set of pre-defined cell conditions determined from limb path tangent segments for each shell. Each ray is modeled by partitioning the optical mass into segments with mass-weighted pressures closely approximating the pre-defined cell pressures. For multiple limb raypath applications the number of cross section calculations is

reduced by a factor equal to the number of shells. This technique is faster and usually more accurate than interpolation of cross section over pressure.

Although this procedure greatly reduces the number of cross sections required, the mass-weighted temperatures of non-tangent path segments may be slightly different than temperatures used in the cross section calculation. Under most conditions this causes minimal (much less than 1%) error. However, for large layers with steep thermal gradients or highly temperature sensitive spectra, this may lead to errors as high as several percent. In such cases, either smaller layers should be used or a more exact mass calculation scheme should be selected.

The second optional model uses the more exact mass partitioning of the general mass model but requires cross sections to be calculated for two subsets of cells (i.e., twice the number required by the first optional model). This option originated from the observation that mass-weighted temperatures and pressures vary only slightly for non-tangent path segments from one ray to the next over the same atmospheric layer. The mass-weighted values of non-tangent path segments are closely approximated by a linear path through a plane parallel atmosphere. Path weighted
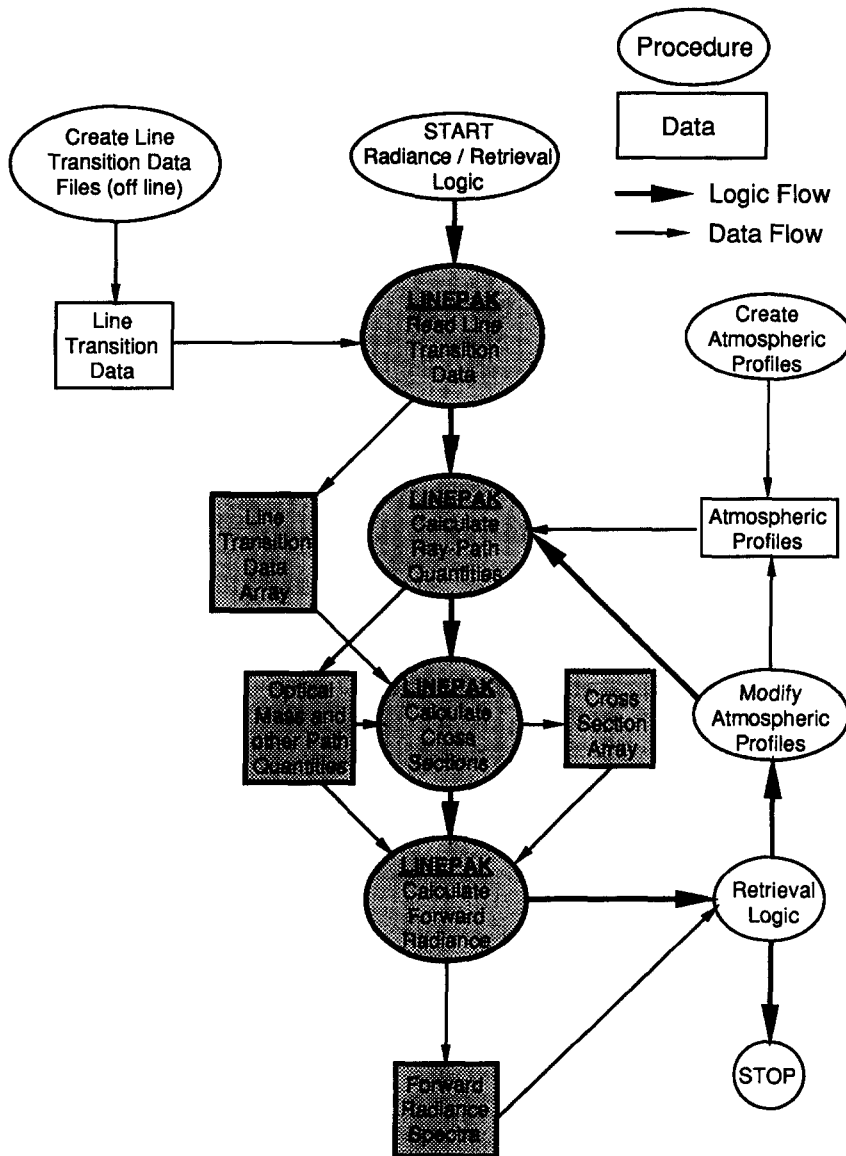

Fig. 8. Typical data and logic flow for retrieval application. Shaded objects indicate LINEPAK modules or output.
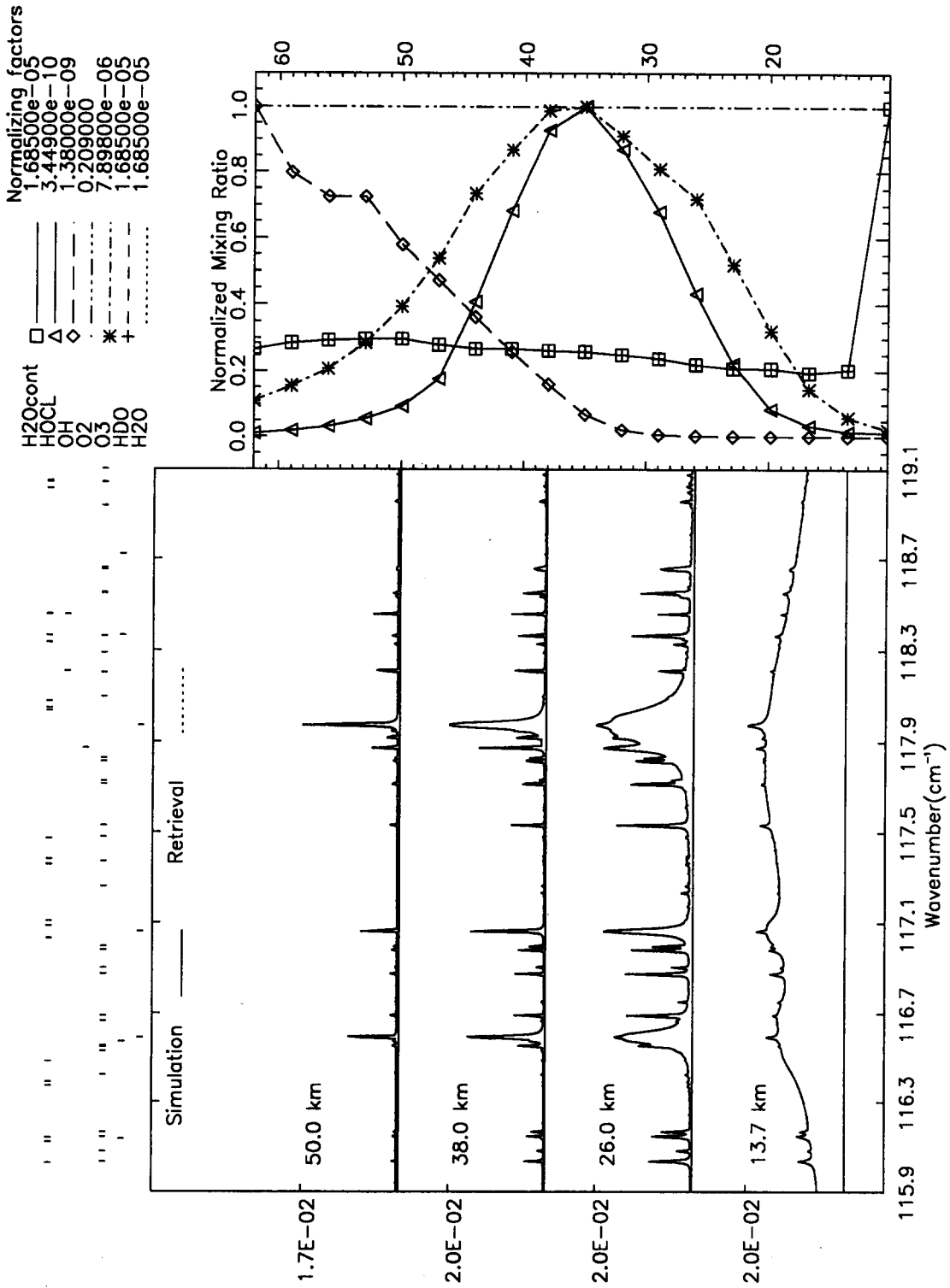
Fig. 9. Interferometer data processing simulation. Selected spectra for 4 of 18 rays, species profiles. and line positions.
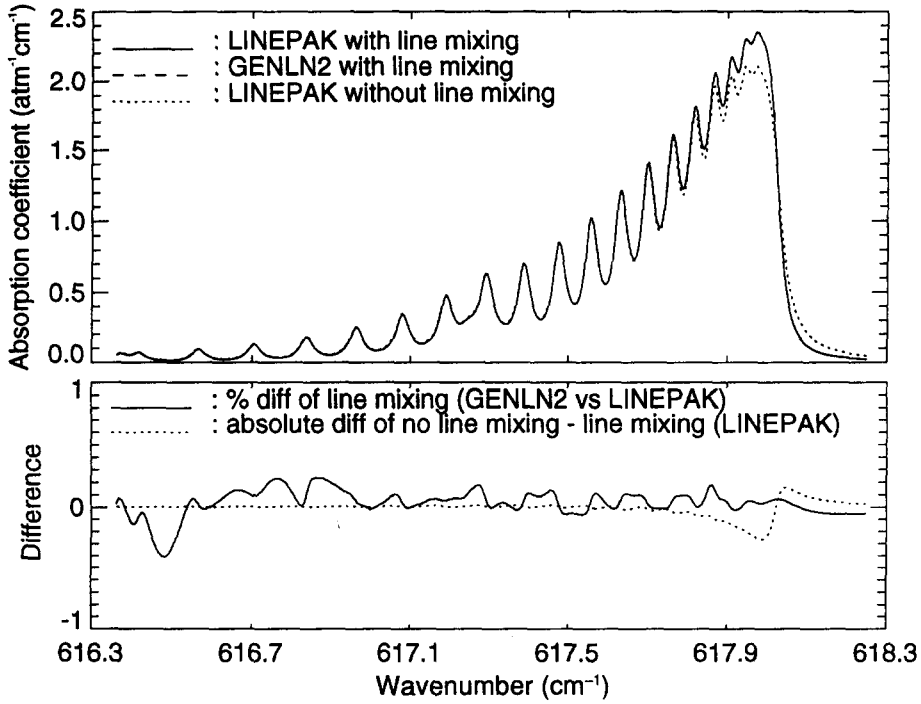
Fig. 10. Comparison of CO_2 Q-branch calculations.

quantities through a parallel layer are the same regardless of the linear path. Thus, cross sections are calculated for each atmospheric layer (shell) for two sets of conditions: (1) tangent cell conditions and (2) non-tangent cell conditions. Although this is twice the number of cross sections
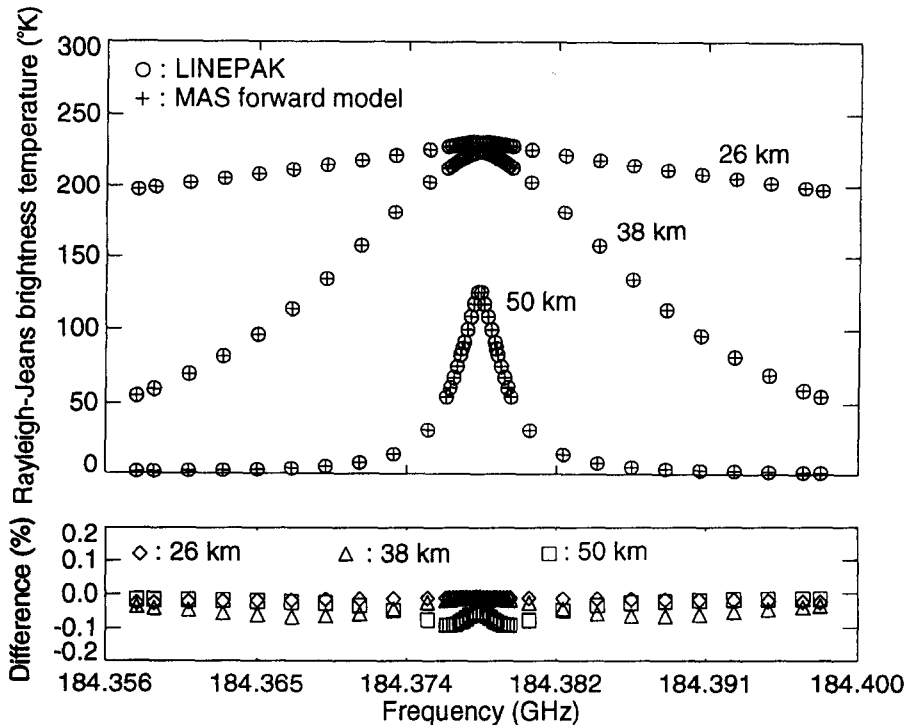

Fig. 11. Comparison of limb calculations with NRL MAS model. Single spectral line for 3 tangent rays.

as required for the first optional model, it is still much less than the number required for full implementation of the general method that treats every segment as an independent cell, and is nearly as accurate. Since path, cross section, and integration routines can be used separately, other schemes can be developed that model large sets of segments with subsets of cell conditions.

6. PATH INTEGRATION

LINEPAK provides procedures for total raypath integration of radiance and transmission which take advantage of the spectral and spatial partitioning methods discussed in the previous sections. Almost any realistic observation geometry may be modeled using these procedures. Special path integration procedures are included to facilitate limb path onion-peel retrieval applications by saving appropriate transmission and radiance spectra for numerically efficient iteration of optical mass. Segment parameters and cell spectra are readily available for incorporation into custom integration schemes, if desired.

6.1. Generalization of observation geometry

The cells (and corresponding ray segments) are numbered using a scheme that facilitates piece-wise operation along the path. An observation geometry is defined by selection of platform altitude and apparent tangent altitude (negative tangent altitude indicates that the raypath intersects the earth) or view angle. Observed radiance is then modeled by selection of the path segments to be integrated. For example, to model a limb path observation from space at point (A) in Fig. 1, the inputs would specify a platform altitude external to the atmosphere (exo-atmospheric), an apparent tangent altitude at the lower edge of shell 3 and request integration from segments -1 to 1. To model a nadir observation of the Earth's surface from point (B), the user would again specify an exo-atmospheric platform altitude, an apparent tangent altitude of $-R_E$ (the radius of the Earth) and request integration from segments -1 to 5, or -1 to -4 to include only atmospheric layers. This scheme allows specification of full rays, subrays and segments, facilitating use with scattering models. All calculated values associated with segments are made available to higher level code through output arrays, allowing custom integration schemes and source functions.

6.2. Integration techniques

Integration of path radiance and transmission is performed in one of two ways. The most memory efficient is integration from the innermost cell (tangent cell for limb calculations) to the outermost cell. A more numerically efficient procedure for limb viewing onion-peel applications is integration from outermost cells to the tangent cell. This allows updating the total ray by simply recalculating the tangent layer transmission. Since these two methods are conceptually similar, only the second method will be discussed in detail. For calculation of raypath transmission, optical depths at each spectral point are summed over the raypath and the exponential in Eq. (3) is calculated once per ray per spectral point. Updating transmission simply requires updating the optical depth sums and repeating the exponential operations. Emission calculations are more lengthy. However, updating total ray emission radiance for an onion-peel retrieval can be performed with only a fraction of the calculations required for a total ray calculation. The integration is performed at every spectral point from the outer cell toward the inner cell as depicted in Fig. 7. Values of radiance and transmission are independently accumulated for two half rays. One half is from the outer cell on the instrument side (near side) of the tangent point to the tangent point. The second half is from the outer cell (far side) to the tangent point.

Although not depicted in the three layer example in Fig. 7, the top layer is used to approximate the entire atmosphere above the first shell boundary. Conditions of temperature and volume mixing ratio are assumed constant above that point and pressure is defined by hydrostatics. To reduce the small error caused by this approximation, additional shells can be defined.

Starting from the outer cell we define the monochromatic radiance contributed by the outer cell on the near side as

$$L_n(1) = [1 - t_n(1)]B_n(1)$$

where $t_n(1)$ and $B_n(1)$ are the cell transmission and Planck value respectively. The radiance from the outer cell on the far side, unattenuated by the intervening atmosphere, is

$$L_f(1) = [1 - t_f(1)]B_f(1).$$

The near side and far side total transmissions, τ_n and τ_f respectively, are initialized to the outer cell transmissions, $t_n(1)$ and $t_f(1)$.

Transmissions and radiances are then accumulated for subsequent cells by the recursive relations

$$\tau_n(j) = t_n(j)\tau_n(j-1)$$

$$L_n(j) = L_n(j-1) + B_n(j)[\tau_n(j-1) - \tau_n(j)]$$

$$\tau_f(j) = t_f(j)\tau_f(j-1)$$

$$L_f(j) = t_f(j)L_f(j-1) + B_f(j)[1 - t_f(j)].$$

At each step of the recursion, the cell transmissions, t_n and t_f, are determined at each spectral point by Beer's law. Completing this process through the tangent layer cell (i.e., to the tangent point, J), the transmission and radiance of the total ray with application of the instrument function, F, is then given for each spectral point by

$$\tau_{total} = \tau_n(J)\tau_f(J)F$$

and

$$L_{total} = [L_n(J) + L_f(J)\tau_n(J)]F.$$

Subsequent updates due to change in the tangent layer conditions only require recalculation of $t_n(J)$ and $t_f(J)$ to use with $\tau_n(J-1)$, $\tau_f(J-1)$, $L_n(J-1)$, and $L_f(J-1)$ which are retained in memory. Also note that multiple instrument response functions, F's, can be applied to simulate multiple channels without repeating spectral calculations. The code allows different values of transmission and Planck temperature on the two sides of ray. This permits application of horizontal temperature and volume mixing ratio gradients when necessary (e.g., sometimes required for polar vortex models).

Although we have described a limb path integration procedure, any portion of a ray can be integrated, allowing a complete range of geometrical cases. All cases are modeled as a complete limb or a section of a limb path.

7. EXAMPLES

Several examples are presented in this section which show both the utility and accuracy of LINEPAK. The most complex of these examples is the simulated retrieval of atmospheric parameters using high resolution spectral data calculated from simulations of space based Earth limb path observations. Other examples include comparisons to line-mixing calculations performed by independent code and comparisons to microwave calculations performed by independent code.

7.1. Limb path simulations

An example which demonstrates the feasibility of simultaneously retrieving all major contributing emitters from high resolution spectral data is given of a study for SAFIRE (Spectroscopy of the Atmosphere using Far Infrared Emission, a high resolution Fourier transform interferometer proposed for the Earth Observation System). The techniques used to perform this study have been applied to independent feasibility studies of several other orbital sensors including HALOE, LIMS, MLS, and CLAES. These studies are of complete limb profile retrievals using the LINEPAK code for rigorous forward calculations.

A multiple-channel, multiple-gas onion-peel retrieval (Marshall and Gordley[14]) has been applied to a feasibility study for SAFIRE. A flow chart of the use of LINEPAK in the retrieval procedure is shown in Fig. 8. We will present an example of simulated retrievals for a bandpass from 115.9 to 119.1 cm^{-1}. High resolution line by line spectra (generated by LINEPAK) is used as input to an interferometer model which apodizes the high resolution spectra to simulate spectra at an

instrument resolution of 0.005 cm^{-1}. Gases modeled were H_2O, HDO (an isotope of H_2O), O_3, O_2, OH, HOCl, and the H_2O continuum. HDO and the H_2O continuum are both modeled using the same volume mixing ratio profile as H_2O (the HDO line strengths are adjusted by an abundance ratio which is equivalent to using the HITRAN data). Retrievals were performed for all gases simultaneously, effectively using each spectral point as an independent channel (O_2 is considered a known constant). To achieve statistical significance, retrievals were performed on 10 different random noise cases with mean noise of zero and standard deviation determined from a signal to noise of 210 relative to a 250 K blackbody.

Figure 9 shows an overlay of simulated and retrieved radiances for several limb paths and one noise case. Also shown are positions of the strongest lines for each gas and the simulated gas volume mixing ratios. The difference between simulated and retrieved radiance is not discernible on the scale shown. Slightly negative points are due to noise applied to the simulated spectra and also to artifacts of the apodization on both simulated and retrieved spectra. The strongest lines in the spectra are the H_2O lines. These lines clearly exhibit pressure broadening at the lower altitude limb paths. The H_2O continuum dominates the spectra at the lowest altitudes. The curved spectral shape at the lowest altitudes is due to use of a Gaussian instrument bandpass function.

A complete set of spectra calculated for 18 limb paths (342 path segments) with all the gases in our example took 105 sec on an IBM RISC 6000 model 550 (rated at 25 megaflops). The retrieval of all gases from simulated noisy spectra required 470 sec on the same machine. The high resolution spectral grid contained 92198 points and used 1750 transitions. These times include no attempt to tune accuracy, filter lines or minimize spectral regions used in the analysis. The retrieval used the path integration method discussed in Sec. 6.2 to minimize updating of total ray radiances due to tangent segment change. The first option discussed in Sec. 5.2 was used for the mass model. Each iteration of the retrieval also required apodization to instrument resolution.

7.2. Line mixing

The line mixing of the CO_2 Q-branch at 617 cm^{-1} is calculated with LINEPAK and compared with GENLN2 (Edwards[2]) calculations in Fig. 10. A set of line mixing parameters from Strow[15] were used. The effect is important for retrieving atmospheric temperatures in the lower stratosphere (Rinsland and Strow,[3] Edwards and Strow[16]). The CO_2 line mixing calculations have been used in support of ISAMS and CLAES, instruments aboard UARS (Upper Atmosphere Research Satellite).

7.3. Microwave spectrum

The brightness temperature derived using LINEPAK is compared with the MAS forward model[17] results near 184 GHz (~ 6.15 cm^{-1}). Figure 11 shows the comparison of brightness temperature for a single ozone line centered at 184.3772 GHz at approximately 26, 38, and 50 km altitudes. The comparisons of calculated brightness temperatures at various altitudes show less than 0.1% differences for full independently calculated limb paths over altitudes from 10 to 62 km. [Comparisons of absorption coefficients (not shown) between the LINEPAK and MAS forward models give less than 0.02% differences for all pressures and temperatures considered]. It should be noted that the Voigt function is used by LINEPAK. The line shape used by the MAS forward model is the Voigt function where the Lorentz halfwidth is smaller than 48 times the Doppler halfwidth and the van Vleck-Weisskopf line shape elsewhere. Although the van Vleck-Weisskopf line shape should be used at lower altitudes, the comparisons show that this makes little difference for this case.

8. CONCLUDING REMARKS

We have described a set of routines (LINEPAK) that are used as basic modules for building multiple gas and multiple path atmospheric transmission and radiance models. The routines include features that give a very high degree of model flexibility, allowing control of spectral resolution, layering, broadening functions, gas constants, and partition functions. This translates to the benefits of fast (few man hours) configuration to new applications, accommodation of changing

physics, and control of accuracy. Spectral models of atmospheric molecular absorption/emission measurements can be assembled for nearly any instrument in a few hours.

These routines have been used in support of a variety of remote sensing projects including three limb viewers on UARS. Numerical results have been validated by extensive comparisons to other codes, including GENLN2,[2] FASCOD,[18] and the Naval Research Laboratory code MAS.[17] The current version assumes LTE (local thermodynamic equilibrium). However, the modular form and features have made extension to non-LTE applications simple and straight-forward. A version with non-LTE extensions is currently being tested.

REFERENCES

1. S. A. Clough, F. X. Kneizys, L. S. Rothman, and W. O. Gallery, *SPIE* **277**, 152 (1981).
2. D. P. Edwards, *SPIE* **928**, 94 (1988).
3. C. P. Rinsland and L. L. Strow, *Appl. Opt.* **28**, 457 (1989).
4. L. S. Rothman, R. R. Gamache, R. H. Tipping, C. P. Rinsland, M. A. Smith, D. C. Benner, V. Malathy Devi, J.-M. Flaud, C. Camy-Peyret, A. Goldman, S. T. Massie, L. R. Brown, and R. A. Toth, *JQSRT* **48**, 469 (1992).
5. R. R. Gamache, R. L. Hawkins, and L. S. Rothman, *J. molec. Spectrosc.* **142**, 205 (1990).
6. J. H. van Vleck and V. F. Weisskopf, *Rev. mod. Phys.* **17**, 227 (1945).
7. P. W. Rosenkranz, *IEEE Trans. Antennas Propog.* **AP-23**, 498 (1975).
8. S. R. Drayson, *JQSRT* **16**, 611 (1976).
9. J. Humlicek, *JQSRT* **27**, 437 (1982).
10. F. Schreier, *JQSRT* **48**, 743 (1992).
11. S. A. Clough, F. X. Kneizys, and R. W. Davis, *Atmos. Res.* **23**, 229 (1989).
12. J. J. Orlando, G. S. Tyndall, K. E. Nickerson, and J. G. Calvert, *J. geophys. Res.* **96**, 20755 (1991).
13. B. T. Marshall, L. L. Gordley, and D. A. Chu, *JQSRT* **52**, 581 (1994).
14. B. T. Marshall and L. L. Gordley, "Simultaneous Inference of Multiple Atmospheric Parameters using Multiple Channels of Information," in *Optical Remote Sensing of the Atmosphere Technical Digest* Vol. 5, p. 212 (1993).
15. L. L. Strow, personal communication (1992).
16. D. P. Edwards and L. L. Strow, *J. geophys. Res.* **96**, 20859 (1991).
17. R. M. Bevilacqua and B. J. Connor, personal communication (1993).
18. S. A. Clough, F. X. Kneizys, E. P. Shuttle, and G. P. Anderson, "Atmospheric Radiance and Transmittance: FASCOD2, " in *Proc. 6th Conf. Atmospheric Radiation*, Williamsburg (1986).